Electrochimica Acta, Vol. 31, No. 11, pp. 1359–1368, 1986.
Printed in Great Britain.

0013–4686/86 $3.00 + 0.00
Pergamon Journals Ltd.

REVIEW ARTICLE

ELECTROCHEMICAL FACETING OF METAL ELECTRODES*

A. J. ARVIA, J. C. CANULLO, E. CUSTIDIANO, C. L. PERDRIEL and W. E. TRIACA

Instituto de Investigaciones Fisicoquímicas Teóricas y Aplicadas (INIFTA), Facultad de Ciencias Exactas, Universidad Nacional de La Plata, Casilla de Correo 16 Sucursal 4, 1900 La Plata, Argentina

(*Received* 20 *January* 1986)

Abstract—Electrochemical faceting is a term recently coined to denote the preferred crystallographic orientation of grains in polycrystalline metals developed when they are subjected to periodic potential perturbations of determined characteristics. Electrochemical faceting can also be applied to small single crystal beads resulting from melting polycrystalline metal wires. By properly adjusting the conditions defining the periodic perturbation, the resulting electrode surface acquires different preferred orientations which, depending on the nature of the electrode metal, can be followed either electrochemically through conventional voltammetry in the H and O electroadsorption/electrodesorption potential range, and in upd of different metals, or by scanning electron microscopy. The procedure has already been successfully applied to platinum, gold, rhodium and palladium. Electrochemical faceting involves at least two stages, namely, the initiation stage related to an electroadsorption process and a propagation stage associated with the electrodissolution and electrodeposition of the base metal in the acid electrolyte. Stabilization procedures for the freshly oriented surfaces and roughness development are also considered.

INTRODUCTION

The present state of knowledge concerning the surface structure and energy distribution at solid metal electrodes is rather limited in comparison with their wide use in electrochemistry. Structure and energy distribution at solid electrodes are of the upmost importance particularly in dealing with electrocatalytic reactions. Recent work carried out on single crystal metal electrodes offered new insights into this critical question[1–9]. Likewise, the behaviour of polycrystalline metal electrodes in electroadsorption/electrodesorption processes reveals that the metal surface is susceptible of remarkable changes under certain periodic perturbation conditions [10, 11]. These changes can be voltammetrically followed in the potential range of H adatom and O containing species in acid media for platinum, rhodium, gold and palladium[12, 13]. Thus, under certain preset perturbation conditions the electrochemical faceting of polycrystalline metals can be accomplished. The faceted electrode surfaces are very reproducible and promising for investigating electrochemical reactions on reasonable well-defined electrode surfaces. The present work refers to the development of these new techniques and to physical–chemical aspects relevant for understanding the kinetics and probable mechanism of the electrochemical faceting.

CONCEPTUAL ASPECTS ABOUT THE CRYSTAL STRUCTURE

In dealing with facting of metal electrode surfaces it is convenient to briefly revise some concepts of crystal structure[14–16]. The perfectly regular crystal structures for metal electrodes often assumed in electrochemical systems must be carefully distinguished from the more or less imperfect real crystals that constitute the solid electrodes most frequently used. The ideal structure should be considered as the framework within which the different types of imperfections exist.

A completely regular lattice of atoms already involves itself imperfections caused by the displacement of atoms from their ideal location due to thermal vibration. This wave motion is described by phonons, that are quantized elastic waves. Another imperfection is the electron–hole combination denoted as exciton which is formed in suitable structures when a valence electron absorbs sufficient radiant energy to move from its full Brillouin band to the upper unfilled band. On the other hand, imperfections in the lattice should be considered, namely, point defects such as vacancy, interstitialcy, Frenkel defect and impurity atom, line defects and surface defects.

The two most important structural defects of real crystals are vacancies and dislocations. The former are empty lattice sites and the latter correspond to extended discontinuities in the internal structure. A type of line defect is the edge dislocation. The alignment of many dislocations creates internal surface boundaries in metal structures such as grain boundaries. In the simple cubic lattice a dislocation can be described in terms of a slip plane, that is the plane along which a dislocation moves. The quantitative description of dislocations is given by the Burgers vector. A dislocation usually moves one lattice spacing and on reaching the edge of the crystal or a grain boundary it disappears by producing a unit step of slip. It is also possible for an edge dislocation to convert inside the crystal into a screw dislocation. Components of edge

* This paper is based on the plenary lecture delivered by Prof. A. J. Arvia at the 36th ISE Meeting, Salamanca, Spain (1985).

and screw dislocations jointly originate a closed dislocation loop within the crystal. In more complex structures most commonly encountered such as body-centered cubic, face-centered cubic and close-packed hexagonal the splitting of a dislocation into partial dislocations has to be considered. After these considerations one presumes that a perfect metal single crystal is somewhat a laboratory curiosity. The normal way in which metal electrodes are used is in the form of polycrystalline aggregates, that is, a set of many individual grains of microscopic size. Crystal imperfections in the cold worked state of metallic materials are associated with uniform and non-uniform strains causing grain deformation through residual stress (microstress and macrostress).

The properties of a single-phase aggregate are determined by those of a single crystal of the material and the structure of the aggregate, that is, relative size, perfection and orientation of grains making up the aggregate. Each grain in a polycrystalline aggregate normally has a crystallographic orientation different from that of its neighbours. When the orientation of all the grains tend to cluster to a greater or lesser degree about some particular orientation the condition of preferred orientation is achieved. Then, the polycrystalline aggregate is textured (in volume) or faceted (at the surface level). Therefore, textured or faceted materials should exhibit anisotropic properties as occurs in most single crystals.

METHODS FOR PRODUCING CHANGES IN SURFACE STRUCTURE OF METALS

Non-electrochemical methods

Different non-electrochemical procedures are effective to produce changes in the surface structure of metals. Faceted metal surfaces result, for instance, through an adsorption–desorption cycle of gas molecules; by chemical etching, by thermal treatments or by surface ionic bombardment. Thus, metal surface reconstruction provoked by oxygen adsorption–desorption cycles changes an atomically smooth (111) platinum metal surface to a platinum (111) partially ordered one [17].

Chemical etching of metal surfaces in strong acid electrolytes produces a removal of surface layers including those metal layers altered by mechanical treatment[18]. Depending on the experimental conditions this treatment furnishes the enhancement of faceting of the metal surface. Let us consider as a typical example, the chemical etching of platinum. Thus, after holding platinum foil electrode for 1 min in boiling aqua regia, the etching pattern clearly showed the elongated texture produced in rolling[19]. The etched electrode had a voltammetric response which indicated a higher proportion of weakly bounded hydrogen. Furthermore, in this case etching caused a decrease in the H adsorption voltammetric charge of 10%. This was attributed to the exposure of a higher proportion of crystal planes with a low surface atom density, such as, for example, the (110) surface.

By means of thermal treatments it is also possible to eliminate defects and residual tensions at the surface and, eventually, to change grain size distribution[14]. This thermally faceted surface in the case of platinum can be accomplished by heating in air a platinum piece[20] or in nitrogen at 400°C, a platinized platinum which has been obtained by electroreduction of a thick platinum oxide layer[21].

Changes in surface structure can also be accomplished through ion sputtering[22]. In this way, a polycrystalline platinum surface which has been bombarded by mercury ions under normal incidence furnishes etch hillocks[23]. Likewise, (111) platinum single crystal surfaces after bombardment by argon ions at 1000 eV and 320°C, develop step edges lying along the (110) direction[24].

Electrochemical procedures

Application to polycrystalline metal structures. Electrochemical procedures to modify the polycrystalline electrode surface can be grouped as follows:

(i) Electrodeposition under modulated potential conditions[25].

(ii) Cyclic fast electroformation and electroreduction of thick oxide layers followed by slow electroreduction scan[26, 27].

(iii) Cyclic fast electroadsorption and electrodesorption of hydrogen adatoms and oxygen-containing species at room temperature[10, 11].

(iv) Cyclic potential perturbation at relatively high temperature by using a molten electrolyte[21].

It should be noticed that procedures (i), (ii) and (iv) involve a modification of the electrode surface both in texture and roughness. Conversely, procedure (iii) principally implies preferred orientation effects without any appreciable change in roughness factor. Let us first consider the electrochemical procedures involving changes in the active surface area.

Both the electrodeposition of metals by *ac* modulating a *dc* potential and the pulsating electrolysis at different frequencies offer the possibility of attaining different preferred oriented surface structures depending on the potential limits and frequency of the modulating signal, and on the *dc* potential. These techniques are usually accompanied by a slight modification of the electrode roughness[25].

The second technique was successfully applied to a polycrystalline platinum electrode in 0.5 M H_2SO_4 at room temperature[26]. In this case, the electrode is subjected to a fast square wave potential perturbation at a frequency in the order of kHz with the lower limit (E_l) in the potential range of the hydrogen evolution reaction and with the upper limit (E_u) in the potential range where a thick oxide layer is grown. After the treatment, the oxide layer is electroreduced by means of a slow potential sweep yielding after the complete electroreduction a highly rough surface free of pores. The voltammogram of the resulting electrode surfaces run at 0.3 $V\,s^{-1}$ in the potential range of H and O adatom shows a remarkable increase in the corresponding voltammetric charges and slight changes in the relative height of the current peaks as compared to those of the starting material. The first change is due to the increase in the electrode roughness, whereas the second one is associated with changes in the distribution of the crystallographic planes of the polycrystalline material as revealed by X-ray diffractograms. The new surface structure exhibits a pre-

dominant contribution of (111) planes parallel to the metal surface due to the fast square wave potential perturbation treatment. Similar results are obtained with gold[27], rhodium[28] and palladium[29], except that the distribution of crystallographic planes then depends on the nature of the metal.

Another way of producing similar changes in the surface structure is by applying triangular potential cycling to metals in molten electrolytes. This procedure was applied to platinized platinum electrodes in $KHSO_4$, at 250°C, at 0.04 V s^{-1} in the potential range of the H adatom electrosorption/electrodesorption and double layer charging region[21]. In this case one observes clear changes in going from the voltammogram of the starting material, in 1 M H_2SO_4 at 20°C to that recorded under the same conditions after the electrochemical treatment, namely, a decrease in the active electrode area and a change in the relative height of the H electroadsorption/electrodesorption current peaks. Furthermore, the voltammetric profile run afterwards in the O electroadsorption/electrodesorption potential range is also appreciably changed as is seen in the corresponding peak height to half-width peak ratio. This means that the electrode roughness, the energy distribution of adsorption sites and the ratio of the crystallographic planes were changed by the electrochemical treatment. The global process follows a complex kinetics involving, in principle, short and large range atom rearrangement.

Faceted metal surfaces without appreciable change in roughness are obtained by applying fast potential perturbations such as repetitive square wave potential scanning (RSWPS), repetitive triangular potential sweeps (RTPS) (Fig. 1) or repetitive sinusoidal potential perturbations to polycrystalline metals[10, 30, 31].

The first experiments with this procedure were made with an electropolished polycrystalline platinum wire as starting material[31]. The voltammetric characteristics of the electrode in 1 M H_2SO_4 are determined, at 0.1 V s^{-1}, between 0.05 V and 0.60 V. This voltammogram is taken as reference to follow the extent of faceting reached after applying the treatment described below. The RSWPS program appears as the most suitable for defining the actual potential limits associated with the phenomenon. The influence of the characteristics of the RSWPS treatment on the development of faceting was investigated in the range shown in Table 1.

The degree of development of type (100) faceting of platinum is measured through the h_2/h_1 ratio as derived from the voltammogram run at 0.1 V s^{-1} between 0.05 V and 0.60 V in 1 M H_2SO_4 (Fig. 2) and defined as follows:

$$\frac{h_2}{h_1} = \frac{\text{height of strongly adsorbed H electrooxidation current peak}}{\text{height of weakly adsorbed H electrooxidation current peak}}.$$

The h_2/h_1 ratio for the initial electropolished polycrystalline platinum is *ca* 0.7.

The optimal conditions for type (100) faceting of platinum and the values of h_2/h_1 resulting for different durations of RSWPS (E_l = 0.25 V; E_u = 1.25 V; f = 4.0 kHz) and RTPS (E_l = 0.002 V; E_u = 1.50 V; f = 4.7 kHz) are assembled in Table 2. It is clearly seen that the value of h_2/h_1 approaches to that of Pt(100) single crystal after 12 h RTPS. In this case the corresponding voltammogram results similar to those reported in the literature for Pt(100) single crystal[6, 7].

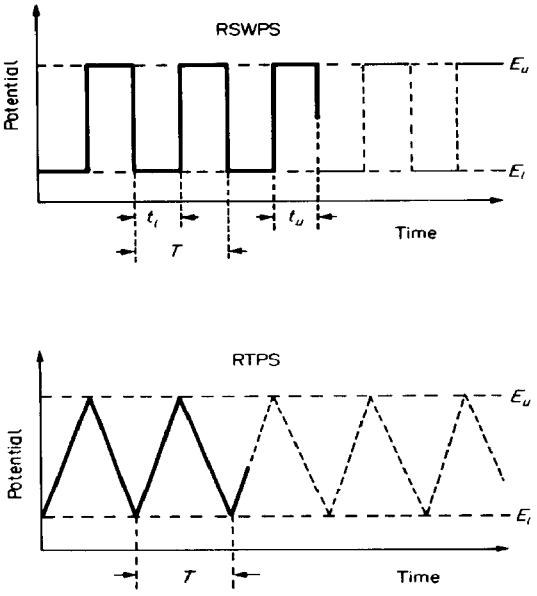

Fig. 1. Typical periodic potential perturbations for electrochemical faceting development. RSWPS = repetitive square wave potential scanning; RTPS = repetitive triangular potential scanning.

Table 1. Range of RSWPS characteristics for producing electrochemical faceting of polycrystalline platinum

0.05 kHz $\leqslant f \leqslant$ 20 kHz
1.0 V (*rhe*) $\leqslant E_u \leqslant$ 1.5 V (*rhe*)
−0.1 V (*rhe*) $\leqslant E_l \leqslant$ 0.7 V (*rhe*)
$0.2 \leqslant (t_u/t_l) = r \leqslant 5$
RSWPS duration: 5 min $\leqslant t \leqslant$ 5 h
(a) Symmetric RSWPS: $t_l = t_u$
(b) Asymmetric RSWPS: $t_l \neq t_u$

Type (111) electrochemical faceting of platinum results when the fast periodic potential perturbation is confined between 0.70 V and 1.40 V. In this case the degree of voltammetric change associated with the (111) faceting can be arbitrarily given by the following ratio:

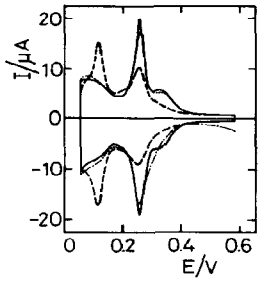

Fig. 2. Voltammograms run at 0.1 V s^{-1} in 1 M H_2SO_4 at 25°C after 4 h RSWPS (E_l = 0.25 V, E_u = 1.25 V, f = 4 kHz). (——) Voltammogram (third cycle) run between 0.05 V and 0.60 V, (–·–) voltammogram obtained after 10 min cycling between 0.05 V and 1.50 V, (– – –) untreated electropolished polycrystalline platinum electrode.

Table 2. Optimal conditions and h_2/h_1 ratio for (100) faceting of platinum. 1 M H_2SO_4, 25°C

h_2/h_1	Conditions	Ref.
6.9	sc	[6]
5.9	sc	[7]
2.2	pc; RSWPS (5 min)	[31]
2.7	pc; RSWPS (4 h)	[31]
4.7	pc; RTPS (12 h)	[56]

sc: single crystal; pc: polycrystal.
RSWPS: E_l = 0.25 V; E_u = 1.25 V; f = 4 kHz.
RTPS: E_l = 0.002 V; E_u = 1.50 V; f = 4.7 kHz.

single crystal and after 30 min triangular potential cycling between 0.05 V and 1.50 V, at 0.1 V s^{-1}, reproduces that described as the "final state" of the Pt(111) single crystal[7, 9, 32]. This situation actually corresponds to a polycrystalline platinum surface[33].

Electrochemical faceting of single crystal metal surfaces. A single crystal metallic sphere offers, in principle, all possible crystallographic planes. When such surface structure is modified by one of the procedures described for the development of preferred orientation, one can obtain a well defined atom arrangement involving a particular crystallographic plane. Due to the spherical geometry, this surface change requires a very symmetrical stereospacial reconstruction[34], which results in the development of poles of the particular enhanced crystallographic plane and the disappearance of others[35].

The above referred changes can be clearly seen by preparing the working electrode from a polycrystalline platinum wire, one of its extremes ending in single crystal sphere made according to Clavilier's method[32]. The initial sphere offers a smooth surface within the range of SEM magnification (×300 to ×15000) standards, involving (111) flattened poles whereas the REM image results in wide terraces with a few atomic steps[36]. The voltammetric response of this spherical platinum electrode in 1 M H_2SO_4 is similar to that already known for any polycrystalline platinum wire. When this sphere is cut in a proper direction and the new surface is put in contact with the electrolyte according to the dipping method[37], the corresponding single crystal voltammogram is obtained[6, 32].

Otherwise, when such a single crystal platinum sphere is subjected to electrochemical faceting to produce a surface whose voltammetric characteristic is assigned to the plane (100), the platinum surface sphere

$$\frac{h_1}{h_2} = \frac{\text{height of weakly adsorbed H electrooxidation current peak}}{\text{height of strongly adsorbed H electrooxidation current peak}}.$$

The optimal conditions for type (111) faceting and the (h_1/h_2) ratio for different duration of RSWPS (E_l = 0.7 V; E_u = 1.4 V; f = 2.8 kHz) and RTPS (E_l = 0.42 V, E_u = 1.10 V; f = 7.4 kHz) are assembled in Table 3. The voltammetric response at 0.1 V s^{-1} between 0.05 V and 0.60 V of the treated electrode surface under the optimal conditions (Fig. 2), can be compared to that reported by Aberdam *et al.*[24] corresponding to "initial state" of Pt(111) single crystal cleaned in UHV (Ar and O bombardment) and characterized by LEED and AES. Nevertheless, the stability of (111) faceted platinum is very sensitive to the parameters of the electrochemical perturbations, as is also the case for Pt(111) single crystal electrodes. Thus, after a single potential sweep between 0.05 V and 1.50 V at 0.1 V s^{-1}, the voltammogram of (111) faceted platinum becomes similar to that described by Aberdam *et al.* as the "standard state" from Pt(111)

Table 3. Optimal conditions and h_1/h_2 ratio for (111) faceting of platinum. 1 M H_2SO_4, 25°C.

h_1/h_2	Conditions	Ref.
1.4	sc	[24, 32]
3.0	sc	[5]
2.0	pc; RSWPS (40 s)	[31]
1.8	pc; RSWPS (5 min)	[31]
2.0	pc; RTPS (12 h)	[56]

sc: single crystal; pc: polycrystal.
RSWPS: E_l = 0.7 V; E_u = 1.4 V; f = 2.8 kHz.
RTPS: E_l = 0.42 V; E_u = 1.10 V; f = 7.4 kHz.

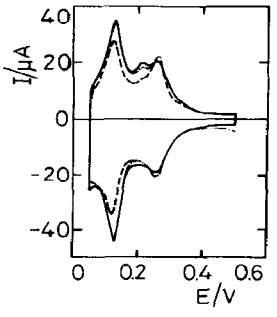

Fig. 3. Voltammograms run at 0.1 V s^{-1} in 1 M H_2SO_4 at 25°C after 5 min RSWPS (E_l = 0.70 V, E_u = 1.40 V, f = 2 kHz). (——) Voltammogram (third cycle) run between 0.05 V and 0.60 V, (–·–) voltammogram obtained after 10 min cycling between 0.05 V and 1.50 V; (– – –) untreated electropolished polycrystalline platinum electrode.

exhibits a dramatic change in the SEM patterns. These patterns show that each pole [100] becomes the origin of four symmetrical and perpendicular bands of steps which develop in the [110] direction to reach the crystallographically equivalent next neighbour pole [100] (Fig. 4). On moving from pole [100] to the direction of pole [111] the surface acquires a faceted kink structure, maintaining cubic geometry.

Equivalent changes can be produced yielding (111) and (110) platinum single crystal surfaces[34]. The corresponding SEM patterns are given as schemes in Fig. 4.

Similar results can, in principle, be obtained by square wave modulated electrodeposition of platinum on a platinum single crystal sphere[38], by using the potential perturbation characteristics reported in a previous work[25].

SEM PATTERNS OF FACETED SURFACES

The stabilized faceted surfaces exhibit SEM patterns completely different to that of the starting material[30]. The most clear patterns are those obtained for (100) faceted platinum. Faceting can be already distinguished with a relatively low magnification (Fig. 5a). The faceted (100) platinum surface exhibits large grains and net grain boundaries with relatively extended straightline portions. Each grain contains a characteristic faceting which exhibits clearly cubic geometry.

The SEM patterns obtained for (111) type faceting are not as clear as those described for (100) type faceting, in correspondence with the voltammetric response already referred to, although in this case the SEM patterns show the definition of grains with a characteristic faceting (Fig. 5b).

ELECTROCHEMICAL FACETING AND ELECTRODISSOLUTION/ELECTRODEPOSITION PROCESSES

Voltammetry, rotating ring disc electrode and thin layer voltammetry data obtained with electrode materials such as platinum, palladium, gold, rhodium, *etc.* in acid electrolyte show that changes in surface topography are associated with the electrodissolution of the substrate itself and electrodeposition of the dissolved metal ion, respectively, during the anodic–cathodic cycles[39]. The steady state rate of platinum dissolution in various inorganic acids is equivalent to 10^{-9} A cm^{-2} at 1.0 V (*vs rhe*) and the rate of the reaction at a constant potential decreases with time presumably due to O electroadsorption[40, 41]. Otherwise, *rrde* measurements of the amount of platinum electrodissolved in $HClO_4$ and H_2SO_4 solutions under RTPS in the 0.45 V to 1.45 V range give

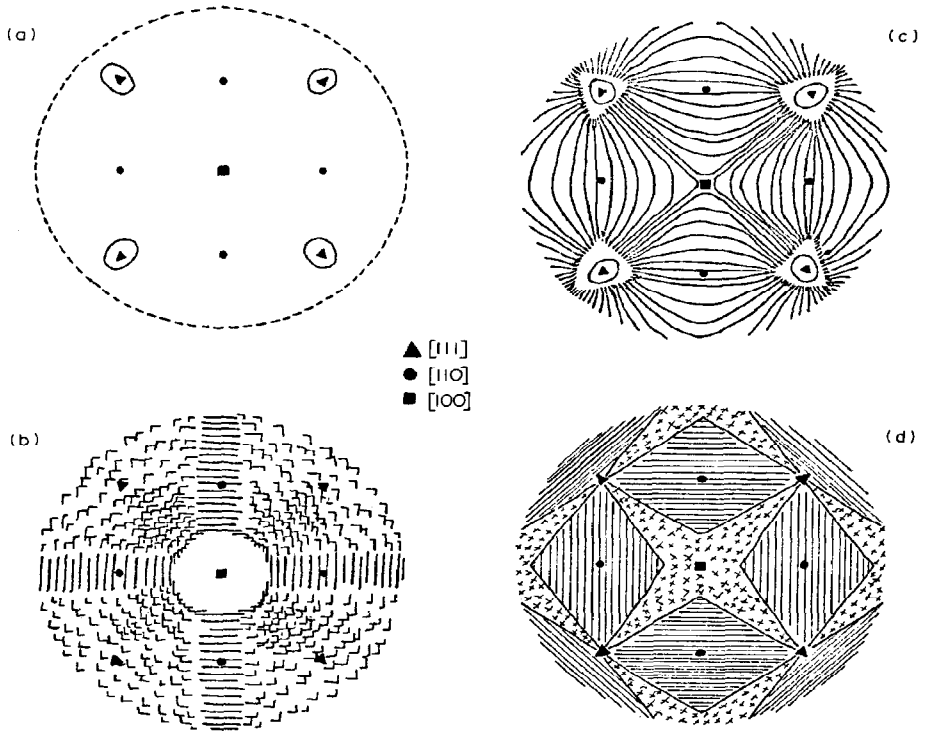

Fig. 4. Scheme of SEM patterns from a single crystal sphere. (a) Untreated single crystal sphere, (b) (100) type faceting, (c) (111) type faceting, (d) (110) type faceting. (Figure reproduced by kind permission of Elsevier Sequoia SA.)

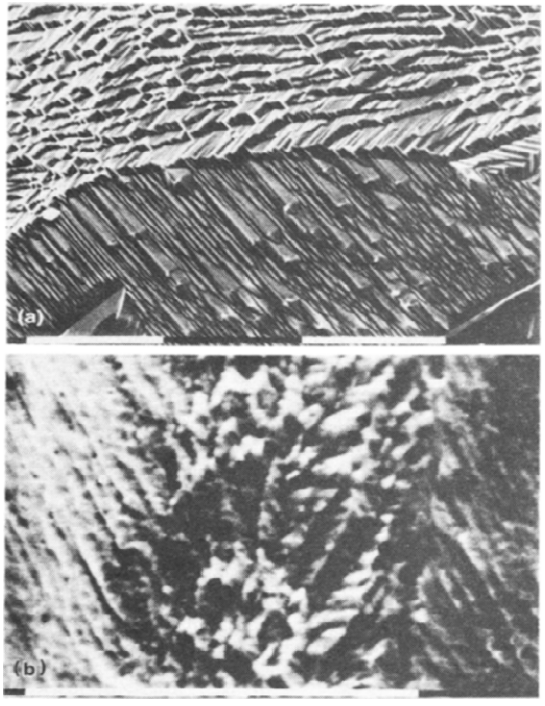

Fig. 5. SEM patterns (scale 10 μm). (a) Platinum surface after 4 h RSWPS ($E_l = 0.25$ V, $E_u = 1.25$ V, $f = 4$ kHz). (b) Platinum surface after 5 min RSWPS ($E_l = 0.70$ V, $E_u = 1.40$ V, $f = 2.8$ kHz).

4.8×10^{-3} μg cm^{-2} on each cycle[42]. Likewise, under RTPS at 40 mV s^{-1} in the 0.41 V to 1.46 V range, platinum dissolution in H_2SO_4 solution amounts 5.5×10^{-3} μg cm^{-2} on each cycle[43, 44].

The experimental procedure to evaluate dissolved platinum produced during the application of the fast periodic potential perturbation consisted of the following three stages[44]: (i) application of the fast potential perturbation (f, ΔE, t) to a polycrystalline platinum in 1 M H_2SO_4; (ii) voltammetric characterization of the treated metal surface at 0.1 V s^{-1} in 1 M H_2SO_4 in the H adatom range; (iii) chemical analysis of soluble platinum species. Measurements were performed by using symmetric and asymmetric RTPS and RSWPS treatments for optimal faceting development.

Runs carried out under the optimal conditions yielding (100) faceted platinum show that the net electrodissolution of the base metal per cycle is 2 to 3 orders of magnitude smaller than that under low frequency potential cycling. Furthermore, the amount of net soluble platinum approaches zero as the duration of the cathodic potential step is increased, whereas when the duration of the anodic potential step is set longer than the cathodic one, the concentration of soluble metal ion in solution approaches that determined under low sweep rate voltammetry. These results, under practically no roughening conditions, furnish evidence that the electrodissolution/electrodeposition processes of platinum during cycling occur restricted to a very thin solution layer adjacent to the electrode and so fast that the fraction of ionic species diffusing out of the metal surface becomes very small.

POSSIBLE EQUILIBRIA AND INTERACTIONS RELATED TO ELECTROCHEMICAL FACETING

Redox process

It is interesting to observe that the electrochemical faceting of platinum yielding either (100) or (111) type surface requires that E_u be positive and that E_l be negative with respect to the potential of the reversible Pt/Pt^{2+} couple (Table 4). Otherwise, the reversible electroadsorption/electrodesorption processes of OH species take place in a potential range lower than that of the equilibrium related to PtO/Pt^{2+} redox couple. Data comprised in Table 4 also show that Pt^{2+}/PtO_2 and Pt/PtO_2 equilibria are thermodynamically feasible in the potential range of the fast periodic potential perturbations which are effective to yield electrochemical faceting.

One should also consider the fact that Pt(II) and Pt(IV) soluble species may also result from the following equilibria

$$Pt(OH)_2 + 2H^+ \rightarrow Pt^{2+} + 2H_2O \quad (3)$$

$$PtO_2 + 4H^+ \rightarrow Pt^{4+} + 2H_2O \quad (4)$$

although no conclusive evidence for Pt(IV) was found.

Nearest neighbour interactions at different sites of the polycrystalline metal surface

Each crystallographic plane should involve its own zero charge potential, as has been clearly estabilished for copper, gold and silver[46–49]. This means that for a certain potential applied to the polycrystalline electrode a true inhomogeneous overvoltage distribution at the surface metal is accomplished which correspondingly, influences in due time the rate of the electrodeposition and electrodissolution reactions. Furthermore, for a particular crystallographic plane the equilibrium conditions at the atomic level for each atom should depend on its position at the crystallographic lattice.

Table 4. Some standard electrode potentials related to platinum[45]

$Pt^{2+}(aq) + 2e^- = Pt(s)$ (1)	$E_1^\circ = 1.188$ V
$Pt(OH) + H^+(aq) + e^- = Pt(s) + H_2O$ (2)	$E_2^\circ \simeq 0.850$ V
$Pt(s) + 2H^+(aq) + 2e^- = Pt(s) + 2H_2O$ (3)	$E_3^\circ = 0.980$ V
$PtO_2(s) + 4H^+(aq) + 2e^- = Pt^{2+}(aq) + 2H_2O$ (4)	$E_4^\circ = 0.837$ V
$PtO_2(s) + 2H^+(aq) + 2e^- = PtO(s) + 2H_2O$ (5)	$E_5^\circ = 1.045$ V

Let us consider for the sake of simplicity a balance of the metal–metal and metal–water interactions playing a part at a cubic lattice site where there is equilibrium between a metal atom at a certain lattice site and the solvated ion in solution. Thus, for a single metal atom in a simple cubic lattice located in three different positions, for example, at a kink, at the plane and at the step edge, the lowest number of interactions playing a part in the electrodeposition process results for a kink atom. On the other hand, one should expect that the electrodissolution reaction occurs preferentially at those sites where metal atoms are more weakly bound to the metal lattice. This should be the case of metal atoms located at grain boundaries in the polycrystalline material.

THE POSSIBLE MECHANISM OF ELECTROCHEMICAL FACETING

The overall process related to electrochemical faceting involves at least two distinguishable stages, namely, the initial stage which occurs at the level of the first O electroadsorbed layer and the propagation stage which corresponds to the three dimensional development of faceting.

The initial stage should be closely related to the electroadsorption of an O containing species, quite likely the electroadsorption of OH on the metal surface through the upd discharge of water. This conclusion is sustained by two facts, namely, that in various metals (platinum, gold, rhodium) the lowest E_u value required to initiate faceting is very close to the threshold potential for upd discharge of water yielding adsorbed OH [Table 4, reaction (2)] and that the reverse of the optimal frequency range for electrochemical faceting coincides with the half-life time of reversible adsorbed OH species on noble metals, which according to triangularly modulated triangular potential measurements, is comprised between 0.5×10^{-3} s and 2.0×10^{-3} s[50, 51].

The OH electroadsorption reaction at site j can be written as follows:

$$(Pt)_j + H_2O = (Pt)_j(OH)_{ads} + H^+ + e^- \qquad (5)$$

Any subsequent reaction yielding irreversible O adsorbed species can be, in principle, disregarded, unless a reversible O adsorbed species is formed. The overall effect of the initial stage is to loose unevenly the metal–metal bond strength at the metal surface through the electroadsorption reaction. In this sense, the initiation of the electrochemical process can be directly compared to the early stages of restructuring of solid surfaces provoked by adsorption of O atoms or molecules from the gas phase[17]. In this respect, it should be mentioned that faceting can be modified just by adsorption of simple molecules as CO or by anion adsorption (chloride ion adsorption on platinum in acid electrolytes)[4, 52]. Independently of the specific action of atoms or molecules, the initial stage concerns with the dynamic behaviour of the solid electrode surface regarding either the adsorption or the electroadsorption process.

The faceting propagation stage is definitely related to the electrodissolution and electrodeposition of the base metal promoted by the fast periodic potential perturbation. The formation of adsorbed OH species actually implies the appearance of a reaction intermediate encountered in the anodic dissolution of most metals in acid aqueous solutions[53]. Therefore, one should expect that a fraction of $Pt(OH)_{ads}$ undergoes electrodissolution yielding soluble Pt(II), according to the following simple formalism:

$$Pt(OH)_{ads} = PtOH^+ + e^- \qquad (6a)$$

$$PtOH^+ \rightleftharpoons Pt^{2+} + OH^-. \qquad (6b)$$

Consequently, during the periodic perturbation reactions (6a) and (6b) together with reaction (5) occur in both directions, their relative contributions depending on E_u, E_l, f and the grade of symmetry of the periodic perturbation. In this respect, the characteristics of the diffusional boundary layer should play an important role in defining the kinetics of the electrodeposition step. This conclusion is sustained by the following facts. The faceting effect produced at a constant frequency and potential limits becomes as a first approximation independent of the shape of the fast periodic potential perturbation. This means that the first harmonics is mainly responsible for the faceting effect. Likewise, the greatest faceting effect is usually observed for symmetric potential perturbation programs. This corresponds to a minimum amount of soluble species in the bulk solution[44]. Therefore, under the fast periodic potential perturbation the average thickness of the apparent diffusional boundary layer (δ_N) should depend on the period (T) of the repetitive potential perturbation according to[54].

$$\delta_N = \frac{c_0}{(\partial c/\partial x)_{x=0}} \simeq \frac{D^{1/2}\tau^{1/2}T^{1/2}}{a} \qquad (7)$$

where D is the diffusion coefficient of soluble platinum, τ is the chronopotentiometric transition time and $a = 0.606$. Therefore, for the frequency threshold ($f = 1.0$ kHz), associated with faceting, $T = 10^{-3}$ s and $D = 10^{-6}$ cm^2 s^{-1}, $\tau = 4 \times 10^{-2}$ s, results in $\delta_N \approx 10^{-5}$ cm. As this average diffusion layer thickness becomes smaller than surface irregularities one should expect a constant diffusion flux at all points of the electrode surface during electrodeposition. Consequently, no roughening should occur.

As a matter of fact for the effective frequency range to develop (100) type faceting of platinum, practically no roughening is observed. This also applies to (111) type electrochemical faceting providing that $f > 2$ kHz. However, in both cases the net electrodissolution per cycle is 2–3 orders of magnitude smaller than under low frequency potential cycling, because platinum electrodissolution/electrodeposition occurs fast and locally so that the fraction of ionic species diffusing out of the metal surface region becomes very small. At the optimal frequencies for preferred orientation the root mean square displacement of dissolved ionic platinum from the surface is in the order of 10^{-5} cm, a thickness value which can be directly compared to δ_N. From the kinetic standpoint the decrease in δ_N means that the polarization concentration contribution for both the electrodissolution and electrodeposition reactions decreases so that the influence of the crystallographic planes in the kinetic response of the electrochemical reaction becomes to a great extent independent of the ambient phase. In this

case, one should expect a selective electrodissolution at grain boundaries of the polycrystalline metal containing weakly bound atoms. Metal atoms at the edge of crystal grains give rise to energy levels which favour OH intermediate formation and metal–metal bond rupture. Hence, the main overall electrodissolution process can be written as follows:

$$\text{atoms at grain boundaries} \rightarrow \text{solvated ions in solution}, \quad (8)$$

although this reaction should not be considered as an exclusive process.

On the other hand, the electrodeposition process implies the formation of definite crystallographic structures where steps are predominantly formed. So the overall electrodeposition can be written as:

$$\text{solvated ion in solution} \rightarrow \text{atoms at kink sites}. \quad (9)$$

Reaction (9) is favoured as it corresponds to a half-crystal atom process which involves the minimum number of metal–metal and metal–water bonds which are broken and reformed during the process. Again the occurrence of reaction (9) as principal does not preclude the participation of other processes. In this respect the electrodeposition process is strictly comparable to electrocrystallization of metals[55], particularly to the formation of stepped crystal faces. The influence of morphology on the kinetics of the electrodeposition reaction has been explained through either a surface diffusion for a step half-distance greater than the average mean free path of the atom at the surface or a direct transfer rate determining step[55]. The crystallographic arrangement attained through electrochemical faceting besides depending on the perturbation parameters is also influenced by any species which can be either adsorbed or electroadsorbed on the metal electrode in the potential range of the fast periodic perturbation. This is the case, for instance, of (100) type faceting assisted by H adatom electroformation at E_l.

As a matter of fact, as the restructuring process proceeds the progressive development of grains with different spatial orientation with stepped surfaces and intergrain boundary regions is accomplished. The definition of the grain boundaries increases according to the duration of the electrochemical faceting treatment. This can be explained in terms of annihilation of defects, such as plane dislocations at the grain boundaries. To some extent the overall process can probably be compared to the motion of an edge dislocation and the production of a unit step at the surface of the crystal.

VOLTAMMETRIC STABILIZATION OF FACETED PLATINUM SURFACES

The voltammetric response of (100) faceted platinum electrodes at low potential sweep rate depends on the potential amplitude range of the voltammetric cycles, the electrolyte composition, the temperature and the adsorption/desorption of foreign substances. Thus, a freshly (100) faceted platinum electrode in H_2SO_4 potential cycled at 0.1 V s^{-1} in the H electroadsorption potential range, approaches a first stable voltammetric condition which corresponds to that of an electrode surface denoted as HASE (hydrogen adsorption stabilized electrode)[52]. The corresponding voltammogram is similar to that previously reported for Pt(100) single crystal under comparable conditions. The voltammetric response of the HASE is also obtained from H and CO adsorption on the freshly (100) faceted platinum electrode surface. The presence of chloride ion in solution during the development of the HASE by potential cycling produces a decrease in the voltammetric charge of H adatoms and a shift of about 0.078 V of the corresponding peak potentials towards more positive values.

A second stage of voltammetric stabilization for (100) faceted platinum results when the electrode is potential cycled at 0.1 V s^{-1} covering the O electroadsorption potential range (anodic switching potential more positive than 0.8 V). This stabilization stage corresponds to an electrode surface denoted as OASE (oxygen adsorption stabilized electrode)[52]. The characteristics of both HASE and OASE can be summarized as follows.

The HASE behaviour requires that $E_u < 0.8$ V. The voltammetric transition from the initial surface to HASE involves an isopotential value at *ca* 0.25 V.

The OASE behaviour is reached for $E_u > 0.8$ V. The voltammetric transition from the initial surface to OASE also involves an isopotential value at *ca* 1.06 V.

The faceted surfaces resulting from the different stabilization procedures remain with the same electrocatalytic properties for a long time either in contact with clean water, clean electrolyte solutions or even in a clean atmosphere of nitrogen. The voltammetric changes related to the stabilization of faceted surfaces correspond to atom rearrangements at the metal surface. Thus, surface rearrangements produced on the (100) faceted platinum electrode in both 1 M H_2SO_4 and 0.5 M $HClO_4$ by potential cycling at 0.1 V s^{-1} and preset E_l and E_u values turn the H adatom voltammogram of HASE into that of OASE, which involves a more even distribution of charge among the various voltammetric peaks.

For both faceted platinum electrodes there is a transition from the "initial state" to the "standard state" of the electrode. This general behaviour of electrode surfaces with defined crystallographic faces suggests that the same common stabilized surface structures are possible starting either from single crystals or polycrystalline metals through restructuring and faceting (Fig. 6). The common structure achieved, as followed through conventional voltammetry, could be assigned to one condition for the solid surface under a crystallographic equilibrium in the absence of residual mechanical stresses[56].

ROUGHENING EFFECTS AT NOBLE METAL ELECTRODES PROMOTED BY ELECTROCHEMICAL PERTURBATION

Nearly two decades ago it was shown that low frequency anodic–cathodic treatments produce changes in surface topography of metal electrodes either in the direction of enhancement of roughnessess or in that of surface smoothing, according to the potential perturbation characteristics[57, 58]. Roughening has

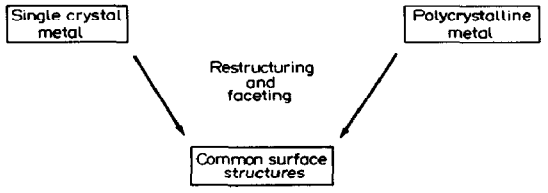

Fig. 6. Simple diagram bridging single crystal and polycrystalline metal surfaces through restructuring and faceting.

been explained in terms of a redistribution of surface metal atoms brought about by forming and breaking Pt–O bonds[58]. It was assumed that more than one O atom was associated with each platinum atom on the anodic step. In this respect ellipsometry data suggest that the second adsorbed O atom resides below the uppermost layer of platinum atoms[59]. This could aid reconstruction of the surface on desorption.

Roughening at low frequency was also attributed to platinum electrodissolution/electrodeposition during cycling[60]. This process is equivalent to surface evaporation and selective condensation and it is expected to produce a clean, fresh metal surface, as is known to occur in surface metal roughening due to adsorption from the gas-phase[61]. However, recent results on polycrystalline platinum have demonstrated that the ability of anodic–cathodic treatments to produce changes in surface topography depend on frequency, symmetry and limits of the periodic perturbation[31]. Thus, depending on these variables three different main effects are accomplished, namely, roughening, sintering or preferred orientation[39, 62].

For polycrystalline platinum in acid electrolyte at room temperature the processes involved in the changes of surface topography and morphology produced by triangular potential cycling in the H and O electroadsorption/electrodesorption potential range at different potential sweep rate can be summarized as follows[62].

Low v ($v < 100\ V\ s^{-1}$): (i) H and O adatom electroadsorption/electrodesorption processes; (ii) platinum electrodissolution/electrodeposition; (iii) long time range sintering. The overall effect produces a slight surface roughening.

Intermediate v: ($100\ V\ s^{-1} \leqslant v \leqslant 1000\ V\ s^{-1}$) (i) H and O adatom electroadsorption/electrodesorption processes; (ii) platinum electrodissolution/electrodeposition. A remarkable surface roughening is produced.

Large v ($v > 1000\ V\ s^{-1}$) (i) H and O adatom electroadsorption/electrodesorption processes; (ii) local platinum electrodissolution/electrodeposition. The prevailing effect is the development of a preferred orientation with practically no surface roughening.

CONCLUSIONS

Both polycrystalline and single crystal metal surfaces during electrochemical faceting develop crystallographic structures approaching the equilibrium form of a crystal which for a given volume (no roughening) implies a minimal total surface free energy. For such ideal structure one should expect a crystal surrounded by flat, atomically smooth, low index faces[63].

The surface modifications induced in single crystal metals by bombardment with high energy particles[23, 24], thermal treatment[17, 24]) and O adsorption from the gas phase[17, 61] are, in principle, similar to those produced by electrochemical faceting treatment. In these cases, the atom rearrangement implies short range and long range energy dissipation effects. The former are principally associated with filling of hole by mobile metastable atoms, mutual annihilation of dislocations and creation of slip planes, whereas the latter comprise the transfer of momentum from the mobile atom to the metal atom network. The metastable metal atoms stabilize in the metal lattice when its translational energy turns into the vibrational lattice energy corresponding to the equilibrium metal structure. The overall process is assisted through selective dissolution and deposition. The stabilization processes may also imply a contribution from surface decontamination which may in turn assist the development of steps and the formation of point defects probably at the grain boundaries.

The penetration of faceting to constitute a preferred oriented metal layer is to some extent comparable to a primary recrystallization where the nucleation and growth of strain-free grains out of the matrix of cold-worked metal takes place[14, 16]. The recrystallized grains usually are not randomly oriented but have their crystal axis lying near certain favoured directions with respect to the cold worked grains. Under some conditions the primary recrystallization is followed by a secondary recrystallization involving a considerable uniform grain growth, produced by a slow migration of grain boundaries. There is no counterpart of the second recrystallization in the electrochemical faceting, although this conclusion is premature as the effect has not been sufficiently studied.

Acknowledgement—This project is financially supported by the Consejo Nacional de Investigaciones Científicas y Técnicas, and the Comisión de Investigaciones Científicas de la Provincia de Buenos Aires. Part of the equipment used in the present work was provided through the Cooperation Agreement between the University of Mainz (Germany) and the University of La Plata (Argentina). This work is also partially supported by the Regional Program for the Scientific and Technological Development of the Organization of American States.

REFERENCES

1. E. Yeager, W. E. O'Grady, M. Y. C. Woo and P. Hagans, *J. electrochem. Soc.* **125,** 348 (1978).
2. A. T. Hubbard, R. M. Ishikawa and J. Katekaru, *J. electroanal. Chem.* **86,** 271 (1973).
3. K. Yamamoto, D. M. Kolb, R. Kötz and G. Lehmpfuhl, *J. electroanal. Chem.* **36,** 233 (1979).
4. P. N. Ross, *J. electrochem. Soc.* **126,** 67 (1979).
5. P. N. Ross, *Surf. Sci.* **102,** 463 (1981).
6. J. Clavilier, R. Durand, G. Guinet and R. Faure, *J. electroanal. Chem.* **127,** 281 (1981).
7. C. L. Scortichini and C. N. Reilley, *J. electroanal. Chem.* **139,** 233 (1982).
8. F. E. Woodward, C. L. Scortichini and C. N. Reilley, *J. electroanal. Chem.* **151,** 109 (1983).
9. F. T. Wagner and P. N. Ross, *J. electroanal. Chem.* **150,** 141 (1983).

10. J. C. Canullo, W. E. Triaca and A. J. Arvia, *J. electroanal. Chem.* **175,** 337 (1984).
11. R. Cerviño, W. E. Triaca and A. J. Arvia, *J. electrochem. Soc.* **132,** 266 (1985).
12. C. L. Perdriel, M. Ipohorski and A. J. Arvia, *J. electroanal. Chem.* in press.
13. E. Custidiano, A. C. Chialvo and A. J. Arvia, *J. electroanal. Chem.* **196,** 423 (1985).
14. A. G. Guy, *Elements of Physical Metallurgy*, Chap. 4. Addison-Wesley, New York (1959).
15. B. D. Cullity, *Elements of X-ray Diffraction*, 2nd edn, Chap. 9. Addison-Wesley, New York (1959).
16. M. D. McLean, *Grain Boundaries in Metals*. Oxford University Press, Oxford (1957).
17. S. Motoo and N. Furuya, *J. electroanal. Chem.* **172,** 339 (1984).
18. C. J. Smithells and E. A. Brandes (Eds), *Metal Reference Book*, 5th edn, pp. 291–363. Butterworths, London and Boston (1980).
19. T. Biegler, *Austral. J. Chem.* **26,** 2571 (1973).
20. T. Biegler, *J. electrochem. Soc.* **116,** 1131 (1969).
21. A. C. Chialvo, W. E. Triaca and A. J. Arvia, *Anal. Asoc. Quim. Arg.* **73,** 23 (1985).
22. M. Kaminsky, *Atomic and Ionic Impact Phenomena on Metal Surfaces*, Springer, Berlin-Heidelberg (1965).
23. G. K. Wehner, *Phys. Rev.* **102,** 690 (1956).
24. D. Aberdam, C. Corotte, D. Dufayard, R. Durand, R. Faure and G. Guinet, *Proc. 4th. Intern. Conf. on Solid Surfaces, Cannes*. Edited by P. A. Degras and M. Costa, Supp. to Le Vide, les Couches Minces, Vol. 1, p. 622. No. 201 (1980).
25. E. Custidiano, T. Kessler, W. E. Triaca and A. J. Arvia, *Electrochim. Acta*, in press.
26. A. C. Chialvo, W. E. Triaca and A. J. Arvia, *J. electroanal. Chem.* **146,** 93 (1983).
27. A. C. Chialvo, W. E. Triaca and A. J. Arvia, *J. electroanal. Chem.* **171,** 303 (1984).
28. A. C. Chialvo, W. E. Triaca and A. J. Arvia, *J. electroanal. Chem.*, submitted.
29. A. E. Bolzan, A. C. Chialvo and A. J. Arvia, *J. electroanal. Chem.* **179,** 71 (1984).
30. R. M. Cerviño, A. J. Arvia and W. Vielstich, *Surf. Sci.* **154,** 623 (1985).
31. W. E. Triaca, T. Kessler, J. C. Canullo and A. J. Arvia, *J. electrochem. Soc.*, submitted. Also *Extended Abstracts*, Vol. 85-1, paper 654, Spring Meeting, The Electrochemical Society, Toronto (1985).
32. J. Clavilier, R. Faure, G. Guinet and R. Durand, *J. electroanal. Chem.* **107,** 205 (1980).
33. F. T. Wagner and P. N. Ross, *Surf. Sci.* **160,** 305 (1985).
34. J. C. Canullo, W. E. Triaca and A. J. Arvia, *J. electroanal. Chem.* **200,** 397 (1986).
35. Y. Uchida, G. Lehmpfuhl, J. C. Canullo and D. M. Kolb, in preparation.
36. Y. Uchida, G. Lehmpfuhl and J. Jäger, *Ultramicroscopy* **15,** 119 (1984).
37. D. Dickertmann, F. D. Koppitz and J. W. Schultze, *Electrochim. Acta* **21,** 967 (1976).
38. E. Custidiano, W. E. Triaca and A. J. Arvia, in preparation.
39. A. E. Bolzan, M. E. Martins and A. J. Arvia, *J. electroanal. Chem.* **172,** 221 (1984).
40. A. N. Chemodanov, Ya. M. Kolotyrkin, M. A. Dembrovskii and T. V. Kudryavina, *Dokl. Akad. Nauk SSSR* **171,** 1384 (1966).
41. A. N. Chemodanov, Ya, M. Kolotyrkin and M. A. Dembrovskii, *Elektrokhimiya* **6,** 460 (1970).
42. D. C. Johnson, D. T. Napp and S. Bruckenstein, *Electrochim. Acta* **15,** 1493 (1970).
43. D. A. J. Rand and R. Woods, *J. electroanal. Chem.* **35,** 209 (1972).
44. C. L. Perdriel, W. E. Triaca and A. J. Arvia, *J. electroanal. Chem.* **205,** 279 (1986).
45. A. J. Bard, R. Parsons and J. Jordan (Eds), *Standard Potentials in Aqueous Solutions*, p. 353. M. Dekker, New York (1985).
46. J. Lecoeur and J. P. Bellier, *Electrochim. Acta* **30,** 1021 (1985).
47. J. Lecoeur, J. Andro and R. Parsons, *Surf. Sci.* **114,** 320 (1982).
48. G. Valette, *J. electroanal. Chem.* **122,** 285 (1981).
49. G. Valette, A. Hamelin and R. Parsons, *Z. phys. Chem.* **113,** 71 (1978).
50. B. E. Conway, H. Angerstein-Kozlowska, F. C. Ho, J. Klinger, B. MacDougall and S. Gottesfeld, *Faraday Discuss. chem. Soc.* **56,** 210 (1973).
51. C. M. Ferro, A. J. Calandra and A. J. Arvia, *J. electroanal. Chem.* **59,** 239 (1975).
52. S. Bilmes, M. C. Giordano and A. J. Arvia, *J. electrochem. Soc.*, submitted. Also *Extended Abstracts*, Vol. 85-1, paper 655, Spring Meeting, The Electrochemical Society, Toronto (1985).
53. A. J. Arvia, *Proc. 8th Int. Congr. on Metallic Corrosion, Mainz*, Vol. 3, p. 2065 (1981).
54. A. R. Despic, in *Comprehensive Treatise of Electrochemistry* (Edited by B. Conway, J. O'M. Bockris, E. Yeager, S. U. M. Khan and R. E. White), Vol. 7, p. 518. Plenum Press, New York (1983).
55. E. B. Budevski, in *Comprehensive Treatise of Electrochemistry* (Edited by B. Conway, J. O'M. Bockris, E. Yeager, S. U. M. Khan and R. E. White), Vol. 7, p. 399. Plenum Press, New York (1983).
56. R. M. Cerviño, W. E. Triaca and A. J. Arvia, *Electrochim. Acta* **30,** 1323 (1985).
57. T. Biegler, *J. electrochem. Soc.* **114,** 1261 (1967).
58. T. Biegler and R. Woods, *J. electroanal. Chem.* **20,** 73 (1969).
59. R. Parsons and W. H. M. Visscher, *J. electroanal. Chem.* **36,** 329 (1972).
60. D. F. Untereker and S. Bruckenstein, *J. electrochem. Soc.* **121,** 360 (1974).
61. J. W. May, *Ind. Engng Chem.* **57,** 19 (1965).
62. R. M. Cerviño, W. E. Triaca and A. J. Arvia, *J. electroanal. Chem.* **182,** 51 (1985).
63. F. C. Frank, in *Growth and Perfection of Crystals* (Edited by R. Doremus, R. Roberts and D. Turnbull), p. 3. Wiley, New York (1958).